

# Influence of building orientation on failure mechanism and flexural properties of LOM specimens<sup>†</sup>

D. Olivier<sup>1</sup>, J.A. Travieso-Rodriguez<sup>2</sup>, S. Borros<sup>1</sup>, G. Reyes<sup>1</sup>, and R. Jerez-Mesa<sup>2\*</sup>

*1 Materials Engineering Research Group, Institut Químic de Sarria, Universitat Ramon Llull, Barcelona (Spain)*

*2 Mechanical Engineering Department, Universitat Politècnica de Catalunya, Barcelona (Spain)*

(Manuscript Received 000 0, 2009; Revised 000 0, 2009; Accepted 000 0, 2009) -please leave blank

---

## Abstract

This paper aims to define the best building orientation for parts manufactured with the laminated object manufacturing technique (LOM), to enhance their flexural performance. Previous research has shown that parts manufactured with LOM have the ability to withstand higher deflections than components created through other layer manufacturing techniques, but, so far, no relation between the building orientation and flexural strength of parts has been assessed.

Four types of specimens have been manufactured, each of them using a different building orientation. They have been tested in a four-loading-points machine to evaluate their failure mode, and extract a conclusion of the best building orientation towards flexural load. 45 degrees was found to be the best building orientation in terms of maximum load before failure. Furthermore, a repetitive failure pattern was found for each tested condition. It is confirmed that building orientation is a relevant parameter in LOM manufacturing with influence on the mechanical properties of parts.

*Keywords:* Flexural strength; Laminated object manufacturing; Layered manufacturing; Rapid prototyping;

---

## 1. Introduction

Additive manufacturing (AM) can be defined as a group of techniques to obtain final parts, prototypes, cores, injection molds for plastics, electrodes for erosion, etc., in a short period of time from a 3D file elaborated with CAD software [1, 2]. As a result of these processes, it is possible to carry out, in a relatively short period of time, different specimens and geometries to validate the definitive design, and to undertake the serial production with reduced development times, and with lower development costs. AM techniques are also often chosen because of the high complexity of parts they can achieve, and the confidentiality they assure when dealing with designs under development. They have also been enhanced through the development of new materials, the improvement of the accuracy of their manufacturing devices, and further simplification of required post-processes, coupled with the extended possibilities that CAD software allow nowadays [3].

Laminated Object Manufacturing (LOM) is one of the mentioned AM techniques. It allows to obtain desired shapes by sticking successive sheets of a certain rolled material. Each layer is cut with a tool, which allows to remove the undesired material, and keeping the necessary volume for the target part [4]. Originally, LOM was used to make laminated paper models [5]. However, as the technique and the availability of

building materials were improved, interest evolved into making functional parts out of metals, ceramics and polymers [6, 7]. Engine components, medical devices and manufacturing molds are some of the parts that can be manufactured through LOM. Previous work has demonstrated that LOM can successfully produce functional parts, for its dimensional accuracy, [8] and low surface average roughness in comparison with other AM techniques [9].

With LOM, parts are manufactured by means of the superposition of thin PVC film layers which are strongly glued to each other by adhesive's jetting trough special adhesive pens. Each layer is formed by cutting with a high precision diamond blade which draws the contour of the part, defining the border between the usable part of the layer and the support material to be discarded. The device, its positioning control systems and dispensing glue system are similar to a traditional printer. When building is completed, a compact layered block is formed. A secondary post-processing operation will be required to peel off the layered support material, so revealing the final part. This post-processing is usually cited as the main disadvantage of this technique [8, 10].

Depending upon the final properties and mechanical characteristics obtained, a rapid prototype can be used as final part, if it is found that its characteristics accomplished with the service requirements of the part. Otherwise, if the mechani-

---

<sup>†</sup> This paper was recommended for publication in revised form by Associate Editor 000 000-please leave blank.

\*Corresponding author. Tel.: +34 934 137 431

E-mail address: ramon.jerez@upc.edu.

cal properties of the part obtained are below the required standards, it still can be useful for design validation of geometrical features, assemblies, ergonomics, marketing analysis, etc. For this reason, performing a characterization of the mechanical properties shown by a part manufactured with any of these techniques is currently of high industrial interest.

Some authors have analyzed the relationship between manufacturing parameters and mechanical properties of LOM-manufactured workpieces. Although most of them focus on the final surface roughness of LOM parts [8, 11, 14], other final properties can be changed by controlling the process building parameters. Among these, building orientation significantly influences productivity factors such as manufacturing time [12]. On the other hand, there is a direct relation between building orientation and the alignment of polymer molecules along the direction of sheet deposition during manufacturing [13]. That is, tensile, flexural and impact strength depend on building orientation in LOM processes. For these reasons, the relation between different building orientations and the resulting flexural properties of LOM specimens has been selected as the main object of study in this paper. The failure mechanism that a LOM bar exhibits under flexural load has been analyzed, in order to have a clearer understanding of the capabilities of this process, and, at the same time, making technological recommendations for workpieces manufactured with a LOM technique working to flexural stresses.

## 2. Materials and methods

A Solid SD300 LOM 3D printer was used to manufacture 80mmx10mmx4mm bars. These flexural test specimens are specified at the ASTM-D790M Standard. The building accuracy of this system is +/- 0.1 mm (XY axis tolerance) and 0.168 mm along the z axis.

As raw material, a laminated SolVC-105 PVC was used. SolGL-101 was the selected adhesive agent and SolAG-154 was the complementary anti-adhesive. Each testing condition had a different building orientation of the deposited SolVC-105 PVC sheet. Four specimens were built for each of these four tested conditions, represented at Fig. 2 and described as follows:

- Specimens #1. Parallel to the x axis. Layers are perpendicular to the loading force.
- Specimens #2. Parallel to the y axis. Layers are perpendicular to the loading force.
- Specimens #3. At a 45-degree angle with the x axis. Layers are perpendicular to the loading force.
- Specimens #4. Parallel to the x axis. Layers are parallel to the loading force.

The flexural properties of the specimens were evaluated with a universal testing machine MTS100. A MTT flexural testing device with four loading points (according to the ASTM D 790M Standard) was used. The calculation and test inputs specified at the standard, shown in Tables 1 and 2, were used for the tests. Four experiments for each building condi-

tion were performed. Experiment 1 refers to each of the bending test performed on specimens #1, and so forth.

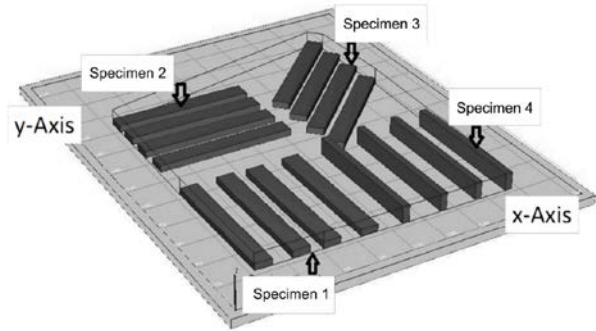


Fig. 1. LOM specimens manufactured under different conditions.

Table 1. Required calculation inputs.

Parameter	Value	Units
Loading Span	21.3	mm
Length of yield segment	2	%
Length of slope segment	2	%
Support span	64	mm
Yield offset	0.002	mm/mm
Point at strain 1	3.5	%

Table 2. Required calculation inputs.

Parameter	Value	Units
Final strain point	3.5	%
Failure sensitivity	90	%
Acquisition data rate	10	Hz
Initial speed	1.9	mm/min

To analyze the failure mechanism of the material, tested specimens were subjected to visual inspection, and failure features were manually measured. Stereomicroscope Leica M60 was used to observe the exhibited crack formation at the specimen layers.

## 3. Results discussion

The specimens were at first tested through a three-point flexural test. A 64-mm loading span was applied, the highest admissible for the selected specimen geometry. No specimen evidenced the presence of failure mechanisms within the deformation range specified at the ASTM D790 standard, so the four bending points test was chosen. It was set up taking 64 mm as support span and a 31.5 mm loading span. A thorough inspection of the tested specimens evidenced a considerable a deformation pattern showing an important component of elastic deformation. The small crack opened at the outer layer had propagated in the z direction, covering the entire thickness of specimens, as shown at Fig. 2. a.

Crack formation was observed at both sides of the specimen. As the parts were opaque, the way this crack penetrated into the inner layers of the specimen could not be observed. Although crack propagation seemed to be superficial, a closer

look at the tested specimens showed a zipper-shaped deeper failure along the transverse section of the parts, as shown at Fig. 2.b. On the other hand, crack propagation showed a different behavior when results of different testing conditions were compared. Some of them evidenced single cracks, and other multiple crack paths. In some cases, those paths were parallel. This first visual inspection procedure evidenced that each set of conditions would result in different crack formation mechanisms, and different number of cracks. In multiple-crack failure specimens, the distance between them was measured, observing a considerable repeatability.

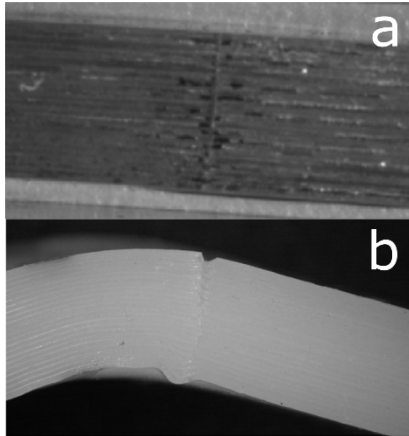


Fig. 2. Failure crack propagation through thickness. a. Cross section of propagated crack b. Detail of specimen failure.

The different macroscopic and microscopic bonding mechanisms of the material affect jointly the global macroscopic behavior of the layered part. At a macroscopic level, the bonding is performed by a chemical adhesive deposited among the different homogeneous layers stacked along the z direction. Internally, the orientation of the extruded PVC sheet molecules favors an anisotropic behavior of the part mechanical properties. It leads to a higher strength along the direction of its orientation, and a lower strength at the transversal direction. Depending on the combination of these two bonding phenomena, different macroscopic responses are expected to be obtained.

**2.1 Specimens #1**

For the tested condition #1, the flexural behavior and failure pattern can be observed in Fig. 3. The average distance between the different propagated cracks, measured on a set of five samples of specimen #1, is shown at Table 3 along with its standard deviation.

Three failure points were observed. One of them was approximately located at the center. This central crack was visually the deepest. The other two failure points coincide with the support points, and were symmetric. The average distance between the different propagated cracks, measured on a set of five samples of specimen #1, is shown at Table 3 along with its standard deviation. In this condition, three failure points

were observed. One of them was approximately located at the center. This central crack was visually the deepest. The other two failure points coincide with the support points, and were symmetric.

In this case, the orientation of the extruded raw material was parallel to the building direction, that is, the longest dimension of specimen is parallel to the building direction, and its layers are stacked to generate the thickness of specimen. It means that when the specimen is loaded, the polymer chains and the bonding adhesive are at the right angles with it.

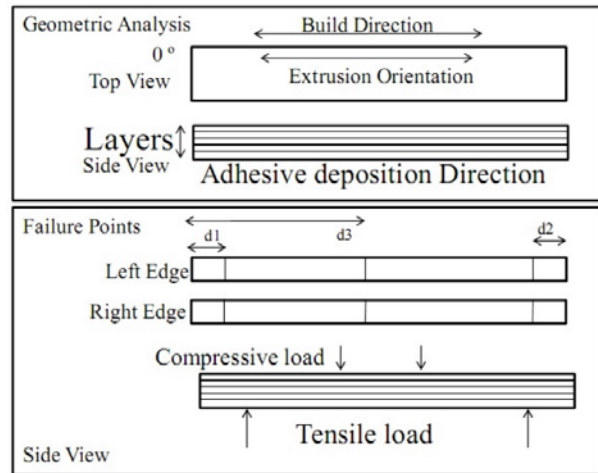


Fig. 3. Schematic representation of failure points for specimens #1.

Table 3. Average values for characteristic lengths of specimens #1.

	Left edge (mm)			Right edge (mm)		
	d <sub>1</sub>	d <sub>2</sub>	d <sub>3</sub>	d <sub>1</sub>	d <sub>2</sub>	d <sub>3</sub>
Mean	9.44	6.54	36.68	9.57	6.63	36.49
SD	0.08	0.37	0.26	0.06	0.20	0.22

**2.2 Specimens #2**

Fig. 4 represents the configuration of the resulting failure mode for specimens #2. Three failure points were observed. One of them was slightly biased from the geometrical center. Two additional failure points were equidistant to it, separated a 20 mm distance from each side. The average experimental values are shown at Table 4. In this case, polymer chains were at the right angles with the longest length of the specimen and the adhesion deposition direction, due to the chosen building direction. On the other hand, the loading device was parallel to the polymer chains orientation, that is, the specimen was loaded along the weakest direction of the microscopic polymer orientation.

Table 4. Average values for characteristic lengths of specimens #2.

	Left edge (mm)			Right edge (mm)		
	d <sub>1</sub>	d <sub>2</sub>	d <sub>3</sub>	d <sub>1</sub>	d <sub>2</sub>	d <sub>3</sub>
Mean	20.69	20.14	38.38	20.44	19.98	38.40
SD	0.25	0.43	0.17	0.59	0.67	0.72

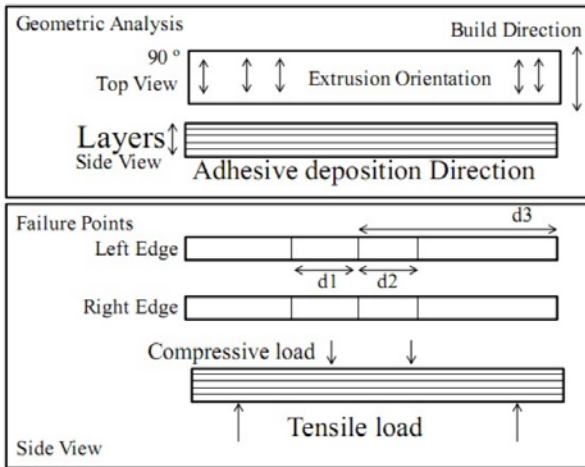


Fig. 4. Schematic representation of failure points for specimens #2.

2.3 Specimens #3

The failure mode of specimens tested at condition #3 is represented at Fig. 5, showing two cracking points. Those points were not symmetric with respect to the top view of the specimen representation, unlike the ones derived from tests #1 and #2. Considering the location of the failure points from one edge to another,  $d_3$  represents the mismatch between cracks observed at both sides of the specimens. Average values are shown at Table 5. Even though the values obtained for failure points,  $d_1$  and  $d_2$ , had a considerably higher dispersion on this test, the obtained gap value  $d_3$  was very consistent.

In this case, the polymer chains, i.e. the strongest direction of the PVC sheet, were oriented at a 45 degrees angle with respect to the longest specimen direction, as a result of the extrusion direction of the stock material. The failure mode of these specimens depicts the way that stresses are concentrated following the direction along which the load is applied. The crack propagates along a direction at right angles with the polymer chains.

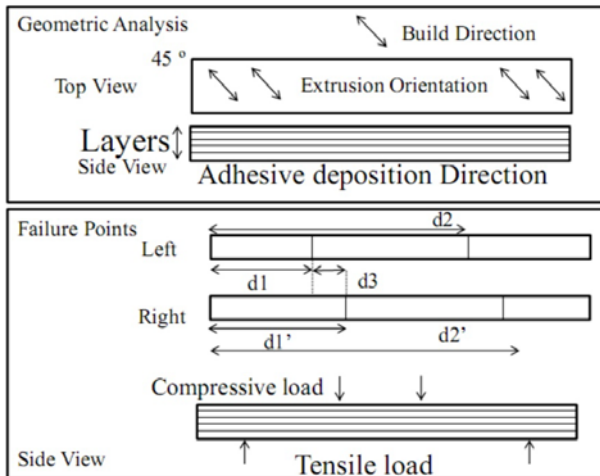


Fig. 5. Schematic representation of failure points for specimens #3.

Table 5. Average values for characteristic lengths of specimens #3.

	Left edge (mm)			Right edge (mm)	
	$d_1$	$d_2$	$d_3$	$d_1'$	$d_2'$
Mean	18.82	47.29	4.72	23.54	51.68
SD	3.74	4.64	0.60	3.97	4.22

2.4 Specimens #4

The results for the fourth set of experiments are shown at Fig. 6. This case showed one single failure point, located approximately at the center of the specimen, and going through the entire thickness showing the mark of plastic deformation. The numerical values measured for the different specimens are shown at Table 6 shown. This testing condition 4 is especially different from the other set of experiments because the loading force is perpendicular to the stacked layers of PVC bound with the polymeric adhesive.

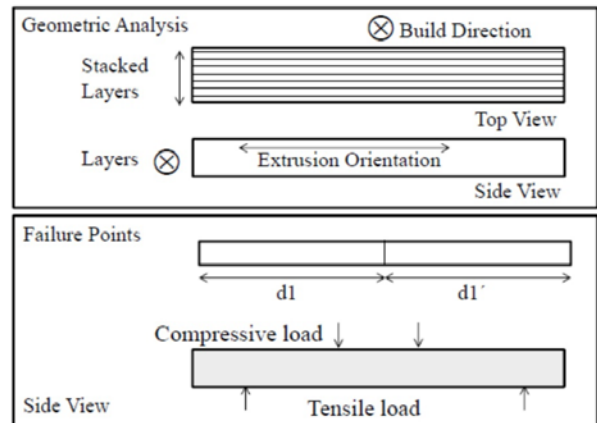


Fig. 6. Schematic representation of failure points for specimens #4.

Table 6. Average values for characteristic lengths of specimens #3.

	up (mm)	down (mm)
	$d_1$	$d_1'$
Mean	39.90	40.05
SD	0.39	0.72

2.5 Flexural curve

After analyzing the four testing conditions, the influence of the macroscopic and microscopic contributions to the bonding of the LOM manufactured parts and their flexural strength, is represented at Fig. 7. Despite the heterogeneous nature of this layered material, the four curves at Fig. 7 show the typical behavior of plastics under flexural load. An initial step of load with pure elastic behavior can be observed, followed by an inflexion region leading to a new plastic-elastic deformation region. At a 3.5% deformation point, the behavior of the four tested conditions is clearly differentiated.

A higher resistance is observed for specimens #3, a lower but very similar strength for specimens #1 and #2, and a considerable lower strength for specimens #4. This behavior is in accordance with the failure points obtained for each set of

specimens, and can be explained as a consequence of the overall contribution of the different bonding mechanisms present internally. At testing condition #3, the influence of adhesive along the z direction of the specimen is combined with the polymer orientation direction orthogonal to the loading force. The higher resistance shown in this case can be understood as a result of the coupled overlapped influences aforementioned.

In the case of testing condition #1, the load is applied perpendicular to the polymer chain direction, which leads to the addition of macroscopic and microscopic contributions, and consequent good resistance properties. The failure mechanism located at the lower supports is due to tensile stress applied to the lower side of the specimen. At condition #2, two failure points besides the central one appear. In this case, the weakest direction of the oriented film is located parallel to the application of load. This explains the defect formation, located close to the loading supports, in which the loaded specimen is mainly subjected to compressive stresses. For condition #4, plastic deformation is reached with lower loads and a lower strength is registered, because of the heterogeneous contributions present in this configuration.

As noted above, specimens manufactured following a 45 degrees from the global axis taken as reference, have a better performance to flexural stresses. This reason is enough conditioning to assert that parts with future similar working regimes should be manufactured keeping this orientation.

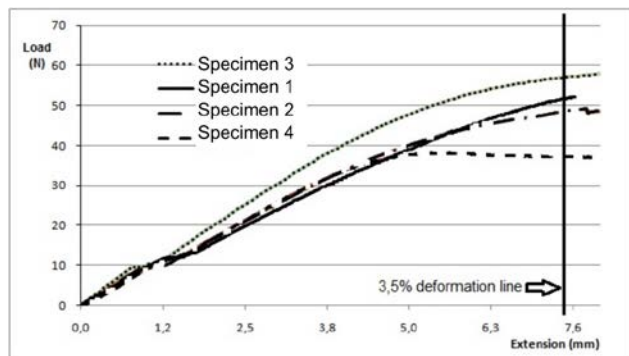


Fig. 7. Flexural curve, according to ASTM D790 standard

#### 4. Conclusions

The contribution of the original manufacturing processing of the stock polymer, and the characteristics of the LOM additive process itself, has shown a combined effect on the macroscopic response expressed in terms of flexural properties. The analysis of the failure mechanism under flexural testing for additive manufactured LOM specimens has shown that:

- Each group of tested conditions shows a repetitive failure pattern. It can be inferred that manufacturing orientation of LOM specimens influences their flexural behavior.

- The stronger direction of LOM parts matches the orientation of the polymer chains due to the stock's sheet extrusion process.

- LOM parts manufactured with a building orientation of 45 degrees present the highest flexural strength.

#### References

- [1] C. K. Chua, C. Feng, C. W. Lee and G. Q. Ang, Rapid investment casting: direct and indirect approaches via model maker II, *International Journal of Advanced Manufacturing Technology*, 25 (2005) 11-25.
- [2] Y. Zhang, X. He, S. Du and J. Zhang, Al<sub>2</sub>O<sub>3</sub> ceramics preparation by LOM (Laminated Object Manufacturing), *International Journal of Advanced Manufacturing Technology*, 17 (7) (2001) 531-534.
- [3] J. J. Beaman, C. Atwood, T. L. Bergman, D. Bourell, S. Hollister and D. Rosen, Additive/subtractive manufacturing research and development in Europe, *WTEC Panel Report* (2004). Consulted online at: <http://wtec.org/additive/report/additive-report.pdf>. Last retrieved on 03/10/2015.
- [4] A. Das, G. Madras, N. Dasgupta and A. M. Umarji, Binder removal studies in ceramic tick shapes made by laminated object manufacturing, *Journal of the European Ceramic Society*, 23 (2003) 1013-1017.
- [5] G. Marchelli, R. Prabhakar, D. Storti, M. Ganter, The guide to glass 3D printing: developments, methods, diagnostics and results, *Rapid Prototyping Journal*, 17 (3) (2001) 187-194.
- [6] Y. Y. Chiu, Y. S. Liao, C. C. Ho, Automatic fabrication for bridged laminated object manufacturing (LOM) process, *Journal of Materials Processing Technology*, 140 (2003) 179-184.
- [7] Y. Shuping, F. Liu, J. Zhang and S. Xiong, Study of the key technologies of LOM for functional metal parts, *Journal of Materials Processing Technology*, 150 (2004) 175-181.
- [8] M. Mahesh, Y. S. Wong, J. Y. H. Fuh, H. T. Loh, Benchmarking for comparative evaluation of RP systems and processes, *Rapid Prototyping Journal*, 10 (2) (2004), 123-135.
- [9] D. Ahn, J. H. Kweon, J. Choi and S. Lee, Quantification of surface roughness of parts processed by laminated object manufacturing, *Journal of Materials Processing Technology*, 212 (2012) 339-346.
- [10] A. P. King Wah and A. Joneja, Geometric techniques for efficient waste removal in LOM". *Journal of Manufacturing Systems*, 22 (3) (2003) 248-263.
- [11] K. Paul, V. Voorakarnam, Effect of layer thickness and orientation angle on surface roughness in LOM, *Journal of Manufacturing Processes*, 3 (2) (2001) 94-101.
- [12] J. Kechagias, S. Maropoulos and S. Karagiannis, Process build-time estimator algorithm for laminated object manufacturing, *Rapid Prototyping Journal*, 10 (55) (2004) 297-304.
- [13] O. S. Es Said, J. Foyos, R. Noorani, M. Mandelson, R. Marloth and B. A. Pregger, Effect of layer orientation on mechanical properties of rapid prototyped samples, *Materials and Manufacturing Processes*, 15 (1) (2000) 107-122.
- [14] J. Kechagias, S. Maropoulos, and S. Karagiannis, Investigation of LOM process quality using design of experiments approach, *Rapid Prototyping Journal*, 13 (4) (2007) 316-323.



**Djamilia Olivier** is a Materials Engineering master's graduate, and expert in 3D printing materials. His field of expertise focuses on the development and validation of new polymeric materials for rapid manufacturing systems.



**Ramón Jerez** is Industrial Engineer and professor at the Mechanical Engineering Department of the Polytechnic University of Catalonia. His research activity tackles with the characterization of rapid prototypes and 3D printed parts, focusing on components manufactured through LOM and FDM devices.